J Orthop Sci (2009) 14:144–149
DOI 10.1007/s00776-008-1310-y

JOURNAL OF
ORTHOPAEDIC SCIENCE

Original article

Scaphoid nonunion and distal fragment resection: analysis with three-dimensional rigid body spring model

Hiroshi Matsuki[1], Emiko Horii[2], Masataka Majima[3], Eiichi Genda[4], Shukuki Koh[5], and Hitoshi Hirata[5]

[1] Department of Orthopedic Surgery, Nishio Municipal Hospital, Nishio, Japan
[2] Department of Orthopedic Surgery, Nagoya First Red Cross Hospital, 3-35 Michishita-cho, Nakamura-ku, Nagoya 453-8511, Japan
[3] Department of Orthopedic Surgery, Yokkaichi Municipal Hospital, Yokkaichi, Japan
[4] Rosai Rehabilitation Engineering Center, Nagoya, Japan
[5] Department of Hand Surgery, Nagoya University Graduate School of Medicine, Nagoya, Japan

Abstract

Background. Distal fragment resection is one of the salvage procedures for scaphoid nonunion with osteoarthritis. Despite being reported as a simple procedure with favorable midterm outcomes, further arthritic changes remain a concern in the long term. Scaphoid waist fracture is classified into volar or dorsal types according to the displacement pattern, but the indications for distal fragment resection have never been discussed for these fracture types.

Method. We reconstructed a normal wrist model from computed tomography images and performed theoretical analysis utilizing a three-dimensional rigid body spring model. Two types of scaphoid fracture nonunion followed by distal fragment resection were simulated.

Results. With volar-type nonunion, the force transmission ratio of the radiolunate joint increased, and the pressure concentration was observed in the dorsal part of the scaphoid fossa and volar part of the lunate fossa of the radius; no deterioration was seen in the midcarpal joint. In the distal fragment resection simulation for volar-type nonunion, pressure concentrations of the radiocarpal joint resolved. With dorsal-type nonunion, force transmission ratio in the radiocarpal joint resembled that of the normal joint model. Pressure concentrations were observed in the dorsoulnar part of the scaphoid fossa and radial styloid. The pressure concentration in the dorsoulnar part of the scaphoid fossa disappeared in the resection model, whereas the concentration in the radial styloid remained. In the midcarpal joint, pressure was concentrated around the capitate head in the nonunion model and became aggravated in the resection model.

Conclusions. With volar-type scaphoid nonunion, distal fragment resection seems to represent a reasonable treatment option. With dorsal-type nonunion, however, pressure concentration around the capitate head was aggravated with the simulated distal fragment resection, indicating a potential risk of worsening any preexisting lunocapitate arthritis.

Introduction

Two types of scaphoid fracture have been outlined by Nakamura et al.[1] One is the volar type, in which the fracture line runs perpendicular to the scaphoid axes and is located at the waist and more distally in the scaphoid. The other is the dorsal type, in which the fracture line displays a horizontal orientation and is positioned more proximally. Moritomo et al.[2] later classified scaphoid waist fractures into two types and then pointed out that each type behaves differently in terms of displacement and associated carpal malalignment according to proximity mapping. The reasons these fracture types show different patterns have not been explained.

Missed scaphoid fractures often progress to nonunion.[3] Treatment should be internal fixation with bone grafting if possible. When nonunion lasts more than 10 years, arthritic changes may develop[4–7] and solid union can be difficult to obtain.

Resection of the distal fragment of the scaphoid nonunion was first reported by Downing in 1951 as a salvage procedure.[8] Several authors have reported favorable surgical outcomes for 2–5 years.[9–11] However, alterations in the load distribution may aggravate arthritic changes in the wrist joint, consequently reducing the long-term efficacy of this procedure. No reports have described the long-term efficacy of distal fragment resection.

The purpose of the present study was to analyze pressure distribution patterns in two types of scaphoid nonunion model using a three-dimensional (3D) rigid body spring model (RBSM) and subsequent alterations in carpal kinetics after simulating distal fragment resection.

Offprint requests to: E. Horii
Received: July 18, 2008 / Accepted: December 2, 2008

Materials and methods

Four healthy women in their twenties without a history of wrist injury volunteered to be the subjects in this study. Informed consent was obtained from all participants prior to enrollment. The wrist joint was scanned with 1-mm intervals by computed tomography (CT) in a neutral wrist position, and a 3D bone surface model was reconstructed from the CT images.

Theoretical analysis was performed using 3D-RBSM. The details have already been reported in the literature.[12,13] With 3D-RBSM, each bone is regarded as a rigid body, and the carpal bones were allowed to displace under simulated load as much as permitted by changes in ligament and cartilage constraints.

In the normal wrist (N) model, orientations and attachments of each ligament were determined from the anatomical literature,[14–18] and 50 ligaments were included in the model. Numbers and stiffness of springs simulating ligaments were determined according to the reported mechanical properties.[19–22] A total of 26 articulating surfaces, with a friction coefficient of 0.001, were constructed in the wrist joint model. The articular cartilage was modeled as a compressive spring with 22.6 N/mm of stiffness. Stiffness of the triangular fibrocartilage complex (TFCC) was assumed to be 5 N/mm.

Scaphoid nonunion was simulated by forming the scaphoid as two rigid bodies with an interposing "rough joint surface" having a friction coefficient of 0.1, which was 100 times higher than that of normal cartilage. We simulated two types of scaphoid waist fracture nonunion (Fig. 1). In the volar-type nonunion model (V model), the fracture line runs perpendicular to the scaphoid axes. Both the dorsal intercarpal (DIC) ligament and the dorsal scapholunate interosseus (d-SL) ligament attach to the proximal fragment. In the dorsal-type nonunion model (D model), the fracture line runs perpendicular to the forearm axes, the DIC ligament attaches to the distal fragment, and the d-SL ligament attaches to the proximal fragment. Distal fragment resection of the scaphoid was simulated on each nonunion model, as the VR model and the DR model, respectively. Resection was simulated by changing the stiffness of the distal fragment from 22.6 to 1.0 N/m, assuming that the space after resection would eventually be filled by scar tissue, the stiffness of which was supposed to be low.

A total load of 140 N was distributed to five metacarpals, simulating the grasp of the hand.[13,23–25] Displacement of the rigid body under this loading can be observed as shown in Fig. 2. Force transmission ratios of the radioscaphoid (RS), radiolunate (RL), and ulnocarpal (UC) joints were calculated; and pressure concentration patterns on each joint surface were also expressed (Figs. 3, 4).

Force transmission ratios and pressure concentration patterns in nonunion and resection models were compared to the normal force transmission pattern. One-factor analysis of variance (ANOVA) was used to test for statistical differences. $P < 0.05$ was considered statistically significant.

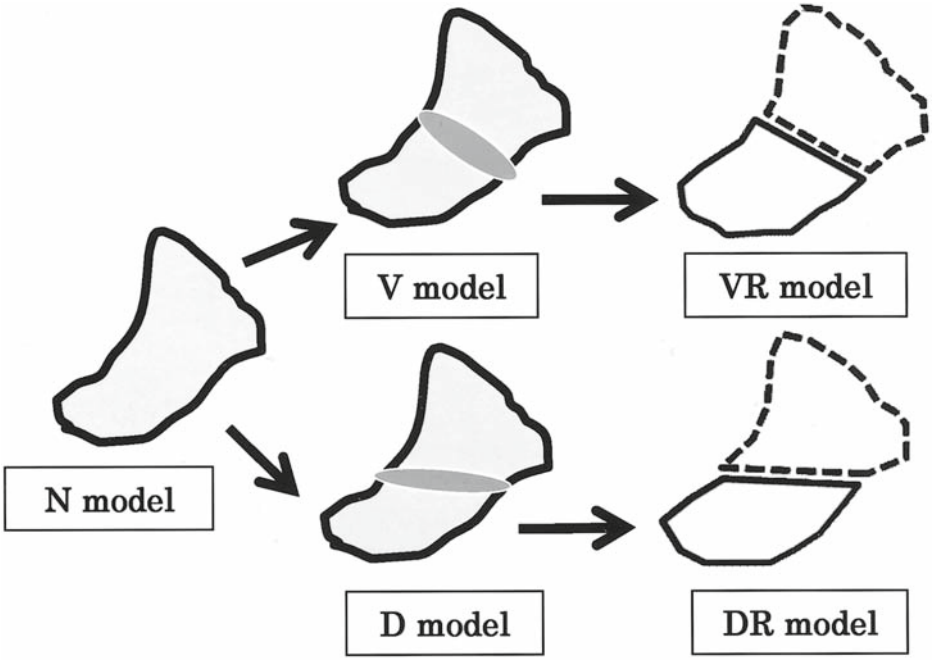

Fig. 1. Simulation of scaphoid nonunion and resection of distal fragments. In the V model, the fracture line runs perpendicular to the scaphoid axis. In the D model, the fracture line runs perpendicular to the forearm axis. On each simulated scaphoid fracture nonunion, resection of the distal fragment was simulated. *N*, normal wrist; *V*, volar-type scaphoid nonunion; *D*, dorsal-type scaphoid nonunion; *VR*, distal pole resection of the volar-type scaphoid nonunion; *DR*, distal pole resection of the dorsal-type scaphoid nonunion

Results

Characteristic changes in force transmission ratio through the radiocarpal (RC) joint were identified after simulation of scaphoid nonunion (Table 1). In the N model, an average force transmission was 47% through the RS joint and 39% and 14% through the RL and UC joints, respectively. In the V model, an average force transmission through the RS joint decreased significantly to 39% (P = 0.018), and through RL joint the transmitted force tended to increase to 46% (P = 0.050), resulting in an inverse distribution within the RC joint compared to the N model. In the D model, force transmission ratio of the RC joint was not significantly changed.

When resection of the distal fragment was simulated, force through the lunate fossa still showed significant increases in the VR model compared to those in the N model, and there was no substantial change compared to the V model. In the DR model, force through the RS joint was significantly decreased compared to that in the N model. These findings are summarized in Table 1.

In the normal wrist, high pressure was observed on the volar area of the lunate fossa and the along the ridge of the scaphoid fossa. In the V model, despite the decreased force transmission ratio of the RS joint, which was equal to the decrease in total force through the scaphoid fossa, pressure concentration was observed at the dorsal edge of the scaphoid fossa. Dorsal rotation of the proximal scaphoid caused pressure concentration on the dorsal rim (Fig. 2). In the VR model, concentrations on both areas decreased. In the D model, concentration was seen on the dorsoulnar part of the scaphoid fossa where the proximal fragment articulated, and on the radial styloid, where the distal fragment sat. In the DR model, the pressure concentration of the scaphoid fossa with the distal fragment resolved (Fig. 3).

At the midcarpal (MC) joint, little change was seen in pressure distribution between the N and V models. However, in the D model, pressure was concentrated

Table 1. Force transmission ratio of the radioulnocarpal joint in each model

Model[a]	Radioscaphoid joint (%)	Radiolunate joint (%)	Ulnocarpal joint (%)
N	47.0 ± 4.5	39.0 ± 6.3	14.0 ± 5.5
V	39.0 ± 2.8*	46.0 ± 4.7***	15.0 ± 7.4
VR	38.0 ± 4.0*	49.0 ± 3.4*	13.0 ± 6.7
D	42.0 ± 3.1	43.0 ± 4.4	14.0 ± 7.1
DR	38.0 ± 3.2**	45.0 ± 5.9	16.0 ± 7.9

Results are given as the average ± SD
[a]N, normal wrist; V, volar-type scaphoid nonunion; D, dorsal-type scaphoid nonunion; VR, distal pole resection of the volar-type scaphoid nonunion; DR, distal pole resection of the dorsal-type scaphoid nonunion
* $P < 0.05$; ** $P < 0.01$; *** $P < 0.1$

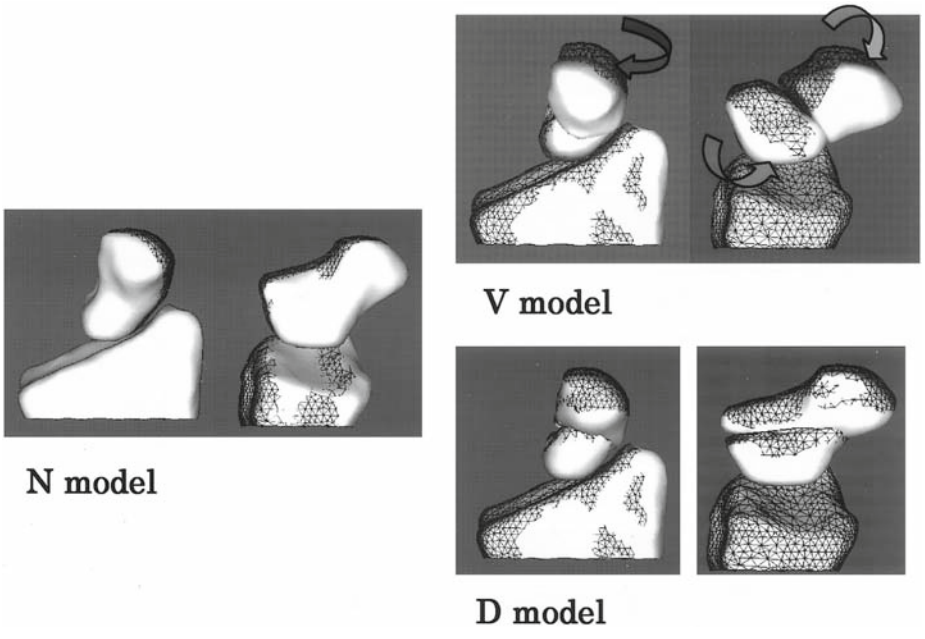

Fig. 2. Displacement of the scaphoid under axial loading

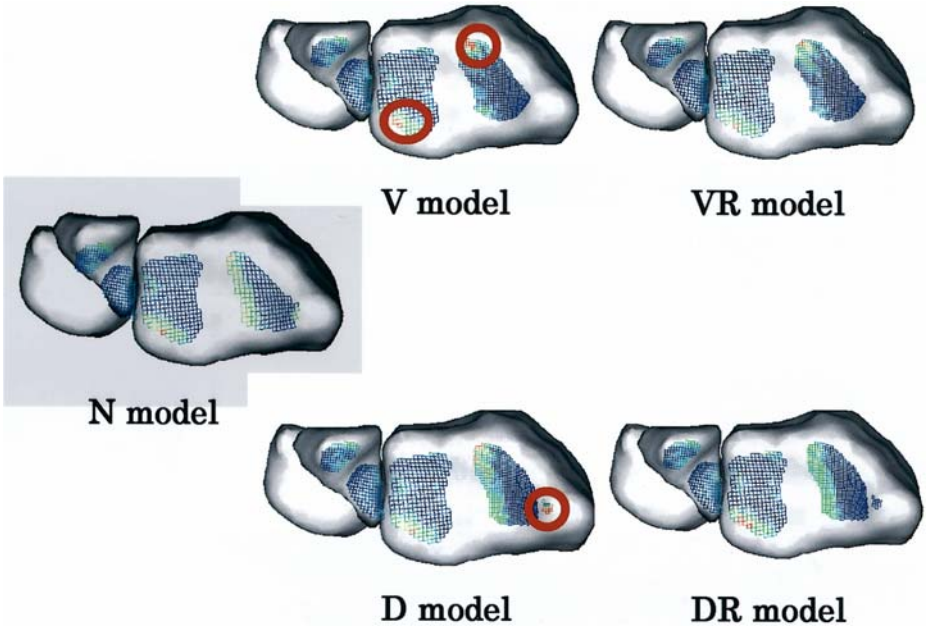

Fig. 3. Pressure concentration in the radiocarpal joint in each model. Pressure > 1 Mpa is expressed as *red circles*

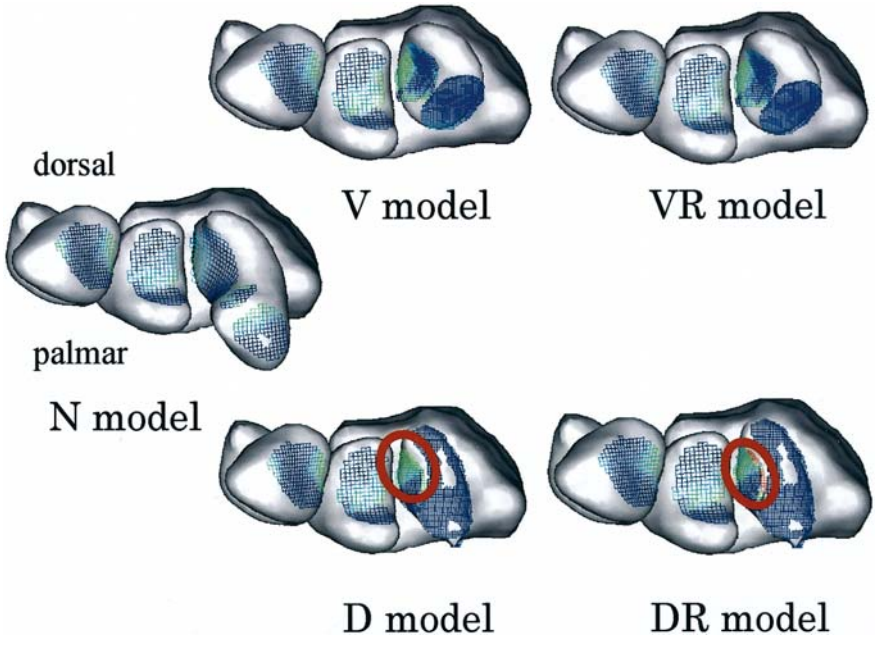

Fig. 4. Pressure concentration of the midcarpal joint in each model. Pressure >1 Mpa is expressed as *red circles*

around the capitate head and concentration was aggravated in the DR model (Fig. 4).

Carpal displacement under axial load is expressed in Fig. 2. In the V model, the distal fragment flexed and pronated, whereas the proximal fragment and lunate extended. In contrast, displacement was subtle in the D model.

Discussion

Fractures of the scaphoid are sometimes left untreated and frequently fall into nonunion.[3] Once established, nonunion can lead to carpal collapse and eventually to wrist arthritis, which may deteriorate wrist function. Nakamura et al.[1] classified scaphoid fractures into volar and dorsal types according to the displacement pattern of the fragments. Moritomo et al.[2] also classified scaphoid nonunion into two types by specifying the benchmark of the fracture line location at the dorsal apex of the ridge. They indicated that the two types of nonunion behave quite differently in terms of the patterns of displacement and arthritic changes observed in patients.

The present study simulated two types of scaphoid nonunion according to Nakamura's classification[1] and

confirmed the different behaviors of the two types of scaphoid nonunion in terms of kinetics. In the V model, the distal fragment flexed and pronated, whereas the proximal fragment and lunate extended, under axial loading. These findings coincide with the humpback deformity and dorsal intercalated segment instability (DISI), which are often observed in volar-type fractures and nonunions. Conversely, in the D model, little displacement was observed between the fragments and adjacent carpal bones. This also corresponded to the clinical observation that DISI and humpback deformity are less frequently observed with dorsal-type fractures and nonunions. Oka et al.[26] analyzed 3D-CT images of scaphoid nonunions and also reported the same pattern of displacements described in the present study.

The natural history of scaphoid nonunion has been reported by several authors. Hidaka and Nakamura[27] noted that arthritic changes first develop at the dorsal ridge and then extend to the radial styloid. During the late stage, arthritic changes develop at the lunocapitate (LC) joint. In our study, different behaviors of the two types of scaphoid nonunion were demonstrated in terms of force transmission ratio in the RC joint. Particularly in the V model, flexion of the distal fragment and extension of the proximal fragment increased force transmission to the lunate fossa. Abnormal pressure concentration between the dorsal ridge and scaphoid might cause early arthritic changes. Conversely, in the D model, the distal fragment created a new pressure concentration on the radial styloid. This might also cause arthritic changes between the distal fragment and radial styloid. Although total force transmitted to the lunate fossa increased, pressure distribution patterns did not show any significant changes, which may explain why the lunate fossa can be spared from arthritic changes after scaphoid fracture nonunion.

Treatment options for salvage of scaphoid nonunion presenting with DISI deformity and/or arthritis have included proximal-row carpectomy, scaphoid excision accompanied by intercarpal arthrodesis, or total wrist arthrodesis. Malerich et al.[9] introduced distal scaphoid resection arthroplasty as a simple and effective procedure.

The scaphoid acts as a link between the proximal and distal carpal rows and forms the radial wall of the midcarpal socket. Distal fragment resection may significantly alter force transmission and kinetics of the wrist. The indications and contraindications for this procedure have been discussed in the literature. Malerich et al.[9] reported favorable outcomes with 2–8 years of follow-up, except in patients with preoperative LC joint arthritis, who experienced aggravation of arthritic changes. Garcia-Elias and Lluch[28] concluded that intercarpal arthrodesis may instead be indicated in cases of preexisting LC joint arthritis, and Soejima et al.[10] reported no progression of arthritic changes postoperatively. Instead, they reported postoperative progression of scapholunocapitate joint arthritis in a patient with type 2 lunate. Conversely, Ruch and Papadonikolakis [11] observed no progression of arthritic changes in patients with a type 2 lunate but found postoperative worsening of the DISI deformity. They concluded that the long-term effects of the procedure on the LC and RL joints were unclear.

All of these clinical reports have described short- to midterm results with small numbers of patients and have thus been inconclusive about the indications and contraindications for this procedure. Biomechanical analysis can provide clues to these problems. In addition, the indications for distal fragment resection have never been discussed according to fracture type.

In the VR model, overall force transmission through the radioulnocarpal joint was unchanged after fragment resection, as the DIC ligament stabilizes the proximal fragment. However, pressure concentration at the dorsal ridge of the scaphoid fossa slightly decreased without any significant alterations in an MC joint pressure distribution pattern. We can recommend resection of the distal fragment for volar-type nonunion, which can resolve the abnormal pressure concentration on the scaphoid fossa without overloading the capitate. On the other hand, in the DR model, although the abnormal pressure concentration disappeared on the scaphoid fossa, pressure concentration over the SC joint increased significantly. Resection of the distal fragment might thus aggravate any arthritic changes in the MC joint.

The DIC ligament has not received much attention in the discussion of distal fragment resection. Ruch and Papadonikolakis [11] emphasized the importance of the SL ligament as functioning regardless of the site of nonunion. Our theoretical analysis demonstrated the importance of the DIC ligament in stabilizing the proximal fragment. Because the VR model showed no pressure concentration, preserving the DIC ligament along with d-SL ligament is recommended in dorsal-type scaphoid nonunion.

Many authors have studied the direct measurement of force transmission through the wrist joint utilizing pressure-sensitive film[29] or small load cells.[30] However, the midcarpal joint has barely been studied owing to the anatomical complexity of the joint and the tight ligament structure. Although several mechanical properties are still unknown, this type of theoretical analysis offers great advantages over direct measurements in studying the complex wrist joints.[31]

There are several limitations in this study. The first, 3D-RBSM is a “static” model simulating only one wrist position. The model also cannot analyze carpal motion with wrist motion, which may affect force transmission

through aggravating abnormal intercarpal motion. Second, the models in the present study were created from normal wrist joints, which therefore cannot take into account long-term changes in carpal alignment and arthritic changes, such as osteophyte formation or ligament attenuation. Simulation using CT of the scaphoid nonunion would provide more accurate simulation of distal pole resection as salvage for long-standing scaphoid nonunion.

No benefits in any form have been received or will be received related directly or indirectly to the subject of this article.

References

1. Nakamura R, Imaeda T, Horii E, Miura T, Hayakawa N. Analysis of scaphoid fracture displacement by three-dimensional computed tomography. J Hand Surg [Am] 1991;16:485–92.
2. Moritomo H, Viegas SF, Elder KW, Nakamura K, Dasilva MF, Boyd NL, et al. Scaphoid nonunions: a 3-dimensional analysis of patterns of deformity. J Hand Surg [Am] 2000;25:520–8.
3. Amadio PC, Moran SL. Fractures of the carpal bones. In: Green DP, Hotchkiss RN, Pederson WC, Wolfe SW, editors. Green's operative hand surgery. 5th edn. Philadelphia: Churchill Livingstone; 2005. p. 713–4.
4. Mack GR, Bosse MJ, Gelberman RH, Yu E. The natural history of scaphoid non-union. J Bone Joint Surg Am 1984;66:504–9.
5. Ruby LK, Stinson J, Belsky MR. The natural history of the scaphoid non-union: a review of fifty-five cases. J Bone Joint Surg Am 1985;67:428–32.
6. Inoue G, Sakuma M. The natural history of scaphoid non-union: radiographical and clinical analysis in 102 cases. Arch Orthop Trauma Surg 1996;115:1–4.
7. Vender MI, Watson HK, Wiener BD, Black DM. Degenerative change in symptomatic scaphoid nonunion. J Hand Surg [Am] 1987;12:514–9.
8. Downing FH. Excision of the distal fragment of the scaphoid and styloid process of the radius for nonunion of the carpal scaphoid. West J Surg Obste Gynecol 1951;59:127–8.
9. Malerich MM, Clifford J, Eaton B, Eaton R, Littler JW. Distal scaphoid resection arthroplasty for the treatment of degenerative arthritis secondary to scaphoid nonunion. J Hand Surg [Am] 1999;24:1196–205.
10. Soejima O, Iida H, Hanamura T, Naito M. Resection of the distal pole of the scaphoid for scaphoid nonunion with radioscaphoid and intercarpal arthritis. J Hand Surg [Am] 2003;28:591–6.
11. Ruch DS, Papadonikolakis A. Resection of the scaphoid distal pole for symptomatic scaphoid nonunion after failed previous surgical treatment. J Hand Surg [Am] 2006;31:588–93.
12. Genda E, Horii E. Theoretical stress analysis in wrist joint: neutral position and functional position. J Hand Surg [Br] 2000;25: 292–5.
13. Majima M, Horii E, Matsuki H, Hirata H, Genda E. Load transmission through the wrist in the extended position. J Hand Surg [Am] 2008;33:182–8.
14. Berger RA. The anatomy of the ligaments of the wrist and distal radioulnar joints. Clin Orthop 2001;383:32–40.
15. Berger RA. The ligaments of the wrist: a current overview of anatomy with considerations of their potential functions. Hand Clin 1997;13:63–82.
16. Nagao S, Patterson RM, Buford WL Jr, Andersen CR, Shah MA, Viegas SF. Three-dimensional description of ligamentous attachments around the lunate. J Hand Surg [Am] 2005;30:685–92.
17. Taleisnik J. The ligaments of the wrist. J Hand Surg [Am] 1976;1:110–8.
18. Mayfield JK, Johnson RP, Kilcoyne RF. The ligaments of the human wrist and their functional significance. Anat Rec 1976; 186:417–28.
19. Schuind F, An KN, Berglund L, Rey R, Cooney WP 3rd, Linscheid RL, et al. The distal radioulnar ligaments: a biomechanical study. J Hand Surg [Am] 1991;16:1106–14.
20. Berger RA, Imaeda T, Berglund L, An KN. Constraint and material properties of the subregions of the scapholunate interosseous ligament. J Hand Surg [Am] 1999;24:953–62.
21. Viegas SF, Yamaguchi S, Boyd NL, Patterson RM. The dorsal ligaments of the wrist: anatomy, mechanical properties, and function. J Hand Surg [Am] 1999;24:456–68.
22. Ritt MJ, Bishop AT, Berger RA, Linscheid RL, Berglund LJ, An KN. Lunotriquetral ligament properties: a comparison of three anatomic subregions. J Hand Surg [Am] 1998;23:425–31.
23. Cooney WP 3rd, Chao EY. Biomechanical analysis of static forces in the thumb during hand function. J Bone Joint Surg Am 1977;59: 27–36.
24. Chao EY, Opgrande JD, Axmear FE. Three-dimensional force analysis of finger joints in selected isometric hand functions. J Biomech 1976;9:387–96.
25. An KN, Chao EY, Cooney WP, Linscheid RL. Forces in the normal and abnormal hand. J Orthop Res 1985;3:202–11.
26. Oka K, Moritomo H, Murase T, Goto A, Sugamoto K, Yoshikawa H. Patterns of carpal deformity in scaphoid nonunion: a 3-dimensional and quantitative analysis. J Hand Surg [Am] 2005;30: 1136–44.
27. Hidaka Y, Nakamura R. Progressive patterns of degenerative arthritis in scaphoid nonunion demonstrated by three-dimensional computed tomography. J Hand Surg [Br] 1998;23: 765–70.
28. Garcia-Elias M, Lluch A. Partial excision of scaphoid: is it ever indicated? Hand Clin 2001;17:687–95.
29. Viegas SF, Tencer AF, Cantrell J, Chang M, Clegg P, Hicks C, et al. Load transfer characteristics of the wrist. Part I. The normal joint. J Hand Surg [Am] 1987;12:971–8.
30. Short WH, Werner FW, Fortino MD, Palmer AK. Distribution of pressures and forces on the wrist after simulated intercarpal fusion and Kienbock's disease. J Hand Surg [Am] 1992;17: 443–9.
31. Iwasaki N, Genda E, Barrance PJ, Minami A, Kaneda K, EYS Chao. Biomechanical analysis of limited intercarpal fusion for the treatment of Kienböck's disease: a three-dimensional theoretical study. J Orthop Res 1998;16:256–63.